



Prediction of Mohr-Coulomb Constants of Selected Korean Rocks Based on Extreme Gradient Boosting Method and Its Evaluation

Seungbeom Choi^a, Hoyoung Jeong^b, and Dae-Sung Cheon^c

^aMember, Disposal Safety Evaluation Research Division, Korea Atomic Energy Research Institute, Daejeon 34057, Korea

^bDept. of Energy Resources Engineering, Pukyong National University, Busan 48513, Korea

^cMember, Geology Division, Korea Institute of Geoscience and Mineral Resources, Daejeon 34132, Korea

ARTICLE HISTORY

Received 3 August 2021
Revised 7 November 2021
Accepted 22 December 2021
Published Online 8 February 2022

KEYWORDS

Mohr-coulomb constants
Prediction model
Extreme gradient boosting
Artificial neural networks
Regression model

ABSTRACT

An accurate understanding of the physical and mechanical properties of rocks is of great importance in several rock mechanical engineering projects. Direct measurement is the most reliable method for obtaining the properties, however, it is sometimes restricted. In such cases, applying prediction models is a practical alternative. The Mohr-Coulomb failure criterion is one of the most frequently adopted models in rock mechanics and is represented by the cohesion and internal friction angle. However, despite their importance, prediction models for the two properties are relatively fewer than those of other properties. In this study, prediction models for the two properties were constructed based on a database collected from southern part of the Korean Peninsula. The extreme gradient boosting method was adopted to construct the models, and their performances were evaluated by comparing them with conventional regression models and artificial neural networks. Consequently, the extreme gradient boosting model exhibited the lowest error and highest prediction performance for both the Mohr-Coulomb constants. In addition, sensitivity analyses were performed to investigate the relative importance of the input variables. This paper aims to provide a database of several properties and to suggest prediction models for the Mohr-Coulomb constants so that it can be utilized as a reference in several rock engineering applications.

1. Introduction

In several rock engineering projects, such as rock slope analyses, deep underground tunnels, and repositories for high-level radioactive waste, it is important to precisely determine the physical and mechanical properties of rocks. Direct measurements by laboratory experiments are the most reliable method to obtain the properties, however, in some cases, they may be restricted when there are budgetary limitations or when there are insufficient rock specimens. Thus, indirect methods, such as, applying empirical prediction models, could be a practical alternative under these circumstances. Various prediction models have been proposed for estimating the relationship between the mechanical and physical properties of intact rock (Horsrud, 2001; Chang et al., 2006; Kılıç and Teymen, 2008; Diamantis et al., 2009), and the relationship between intact and rock mass properties (Nicholson and Bieniawski, 1990; Hoek and Diederichs, 2006; Sonmez et al., 2006), which were deduced

mainly by conventional regression and/or statistical approaches.

Rapid developments in artificial intelligence have led to noticeable improvements in predictions. Artificial neural networks (ANNs) have been used frequently (Singh et al., 2001; Cevik et al., 2011; Ceryan et al., 2013; Torabi-Kaveh et al., 2015), and hybrid or adaptive ANNs, incorporating fuzzy, genetic algorithms have been actively developed (Monjezi et al., 2012; Beiki et al., 2013; Mishra and Basu, 2013; Yesiloglu-Gultekin et al., 2013; Armaghani et al., 2016) to predict rock properties.

Recently, numerous studies and applications have adopted machine learning techniques that are based on the ensemble method. A distinctive feature of the ensemble method is that it makes decisions not based on a single model, but by compiling multiple results from individual basic learners, which is usually in the form of a decision tree. It has drawn attention in several research fields owing to its precision and effectiveness. The ensemble method can be broadly categorized into bagging

(bootstrap aggregation) and boosting methods, and the latter has several strengths in terms of mediating the overfitting problem and robustness (Friedman et al., 2000). Among the boosting methods, extreme gradient boosting (XGB) (Chen and Guestrin, 2016) has been adopted in several applications, such as in the prediction of TBM penetration (Zhou et al., 2021), pillar stability (Liang et al., 2020), blast-induced ground vibration (Ding et al., 2019; Qiu et al., 2021), and properties of geomaterials (Nguyen-Sy et al., 2021; Zhang et al., 2021).

The Mohr-Coulomb failure criterion is one of the most widely used models in the field of rock mechanics, thanks for its brevity and practicality. It determines the failure of the material using a regression line. The failure strengths under different confining pressures are fitted to produce a simple regression and the slope and y intercept of the line represent the internal friction angle and cohesion, respectively. According to the International Society for Rock Mechanics and/or American Society for Testing and Materials (ASTM) standard test methods, at least three to five intact rock specimens are required for a single failure state triaxial compression test (Kovari et al., 1983; ASTM D7012-14e1, 2014). Therefore, triaxial compression test is more time-consuming and costly than other strength tests in terms of the number of specimens, equipment, and testing procedures. Indirect methods for predicting Mohr-Coulomb constants have been developed as well, including regression models (Hajdarwish and Shakoor, 2006; Karaman et al., 2015; Shen et al., 2019) and artificial intelligence techniques (Armaghani et al., 2014; Khandelwal et al., 2018; Shen and Jimenez, 2018). However, despite the importance of these two properties, their prediction models are still fewer than other engineering properties, such as uniaxial compressive strength, Young's modulus, etc.

In this study, the XGB algorithm was applied to establish prediction models for cohesion, and internal friction angle. The models were established based on the database of intact rock properties, which were collected from the southern part of the Korean Peninsula. In order to demonstrate the structure and correlation of the database, statistical analyses were performed first. Thereafter, XGB models were constructed and their performances were evaluated by comparison with other types of prediction models. Regression models and an adaptive ANN, incorporating a simulated annealing (SA) algorithm with a conventional ANN, were established for comparison. Meanwhile, sensitivity analyses were performed to determine the relative importance of independent variables on dependent variables, that is, cohesion and internal friction angle.

2. Algorithm of Extreme Gradient Boosting Method (XGB)

The XGB (Chen and Guestrin, 2016) algorithm is an ensemble method based on gradient boosting, and it has drawn attention because it showed remarkable performance in machine learning competition. After generating multiple bootstrap samples, individual basic learners in the form of a decision tree are sequentially

applied to the samples. In the initial stage, the residual from a tree is calculated and utilized in the subsequent tree as a weight. This update is iterated till all basic learners consider the residuals, leading to a decrease in error because the update takes place along the negative gradient direction. The XGB procedure is explained briefly below. The prediction results, \hat{y}_i of sample the x_i from a decision tree can be defined as in Eq. (1) as follows:

$$\hat{y}_i = \sum_{k=1}^K f_k(x_i), \quad (1)$$

where f_k denotes the score or leaf weight of k -th tree, and K represents the number of trees. A loss function, usually in a quadratic form, can be defined, and the gradient can be presented as well (Eq. (2)):

$$l = \frac{1}{2}(y_i - \hat{y}_i)^2 \quad \frac{\partial l}{\partial \hat{y}_i} = -(y_i - \hat{y}_i). \quad (2)$$

That is, the gradient equals the negative residual, and the entire learning process proceeds in this direction, thereby reducing the residual. As the learning proceeds, the model is updated in a sequence, therefore, the k -th prediction, $\hat{y}_i^k = \hat{y}_i^{k-1} + f_k(x_i)$, is presented in an additive form.

A typical objective function in the XGB algorithm is expressed in Eq. (3):

$$Obj = \sum_{i=1}^n l(y_i, \hat{y}_i) + \Omega(x_i) = \frac{1}{2} \sum_{i=1}^n (y_i - \hat{y}_i)^2 + \gamma T + \frac{1}{2} \lambda \sum_{j=1}^T w_j^2. \quad (3)$$

The first term in the function denotes an ordinary, traditional objective function, whereas the second term is related to regularization. The regularization term is related to model complexity and at the same time, functions as a penalty term to mediate overfitting problems. In the regularization term, γ represents the complexity of the tree, T is the number of leaves in the tree, λ is a penalty constant, and w_j denotes the weight of the j -th leaf node. The loss function in Eq. (3) can be approximated using a second-order Taylor expansion, for simplicity:

$$l(y_i^k, \hat{y}_i^k) = l(y_i^k, \hat{y}_i^{k-1} + f_k(x_i)) = l(y_i^k, \hat{y}_i^k) + \sum_{n=1}^{\infty} \frac{f_k^n(x_i)}{n!} = l(y_i^k, \hat{y}_i^k) + g_i f_k(x_i) + \frac{1}{2} h_i f_k^2(x_i), \quad (4)$$

where g_i , and h_i denote the first and second derivatives of the loss function.

3. Statistical Analyses of Database

Before constructing the prediction models, statistical analyses were performed to demonstrate the characteristics of the database used in this study. The database consists of several properties of intact rock, i.e., specific gravity (SG), porosity (PO), P-wave velocity (V_p), S-wave velocity (V_s), uniaxial compressive strength (UCS), Young's modulus (E), Poisson's ratio (ν), Brazilian tensile strength (BTS), cohesion (c), and internal friction angle (ϕ),

Table 1. Descriptive Statistics of the Database Used in This Study

		<i>SG</i> (–)	<i>PO</i> (%)	<i>V_p</i> (m/s)	<i>V_s</i> (m/s)	<i>UCS</i> (MPa)	<i>E</i> (GPa)	ν (–)	<i>BTS</i> (MPa)	<i>c</i> (MPa)	ϕ (deg)
IGN (n = 205)	Ave.	2.66	1.53	4,428	2,383	138.17	37.57	0.218	11.80	21.27	54.56
	S.D.	0.10	1.69	1,127	579	68.97	18.45	0.050	5.67	9.65	4.81
	Min.	2.37	0.13	1,020	660	13.00	0.70	0.10	1.00	2.00	36.00
	Max.	2.93	9.04	6,600	3,630	321.00	78.59	0.38	29.59	44.90	63.00
MET (n = 394)	Ave.	2.71	0.91	4,392	2,413	115.10	34.40	0.19	11.34	19.51	51.29
	S.D.	0.09	1.14	828	414	53.12	14.37	0.06	4.12	8.22	7.09
	Min.	2.45	0.05	1,160	770	12.00	1.20	0.08	1.00	3.00	35.00
	Max.	3.05	9.04	6,110	3,6680	285.00	69.48	0.36	25.00	50.00	66.00
SED (n = 206)	Ave.	2.68	1.71	4,774	2,564	138.91	35.98	0.20	13.65	23.36	51.28
	S.D.	0.10	1.96	890	450	69.41	13.13	0.05	6.32	10.16	5.38
	Min.	2.40	0.07	1,940	1,180	15.00	3.10	0.10	2.00	4.00	38.90
	Max.	2.91	8.28	6,460	3,610	368.00	77.22	0.33	31.00	57.00	67.00
Total (n = 809)	Ave.	2.69	1.28	4,494	2,441	126.89	35.61	0.20	12.02	20.90	52.15
	S.D.	0.10	1.57	947	477	62.77	15.30	0.05	5.25	9.24	6.32
	Min.	2.37	0.05	1,020	660	12.00	0.70	0.08	1.00	2.00	35.00
	Max.	3.05	9.04	6,600	3,680	368.00	78.59	0.38	31.00	57.00	67.00

Note: Ave., and S.D. denote average, and standard deviation, respectively

which were collected by the Korea Institute of Geoscience and Mineral Resources (KIGAM) in Korea for decades. In order to make the database with no missing values, sets that had all 10 properties were excerpted so that the total number of data sets was 809. Meanwhile, the database was classified roughly by rock type, that is, igneous (IGN), metamorphic (MET), and sedimentary (SED). Table 1 summarizes the descriptive statistics of the database.

In order to investigate the effect of rock type on the properties, a one-way analysis of variance (ANOVA) was performed. In general, the ANOVA result holds true when the samples exhibit normality. Therefore, Kolmogorov-Smirnov (KS) tests were performed first to confirm whether the prerequisite was satisfied. Both normal, lognormal, and exponential distribution were tested simultaneously to find out any possibility of presenting the properties in a form of specific distribution. The results of the KS test revealed that none of the rock types followed the same distribution at the same significance level. Young's modulus was the only property that was fitted by a normal distribution regardless

of the rock type, however, the significance levels of each group were different.

Thus, not all of the prerequisites of ANOVA were strictly satisfied. Nonetheless, the size of each sample (more than 200 in this study) was sufficiently large so that ANOVA, rather than other non-parametric analyses, was performed in a practical attempt. ANOVA normally requires post-analysis to confirm the discrepancies between the averages of each group. If an equal variance could be assumed, the Scheffe criterion was applied as a test statistic and if not, Dunnett's T3 was applied with a 0.05 of significance level for both cases.

Because the assumption of equal variance did not hold under a 0.05 of significance level, Dunnett's T3 was applied to all cases. Within the collected database, cohesion exhibited a difference between MET and SED, while internal friction angle showed differences between all rock types but MET and SED. It could not deduce a consistent trend in the effect of rock types, thus, the effect was not considered in the subsequent statistical analyses as well as in making prediction models. Table 2 lists the ANOVA

Table 2. ANOVA Results of the Cohesion and the Internal Friction Angle

Property	Dunnett's T3				Property	Dunnett's T3			
	<i>i</i>	<i>j</i>	<i>i-j</i>	<i>Sig</i>		<i>i</i>	<i>j</i>	<i>i-j</i>	<i>Sig</i>
<i>c</i> (MPa)	IGN	MET	1.76	0.08	ϕ (deg)	IGN	MET	3.27	0.00*
		SED	-2.09	0.10			SED	3.28	0.00*
	MET	IGN	-1.76	0.08		MET	IGN	-3.27	0.00*
		SED	-3.85	0.00*			SED	0.01	1.00
	SED	IGN	2.09	0.10		SED	IGN	-3.28	0.00*
		MET	3.85	0.00*			MET	-0.01	1.00

*denotes that there exists statistically meaningful differences

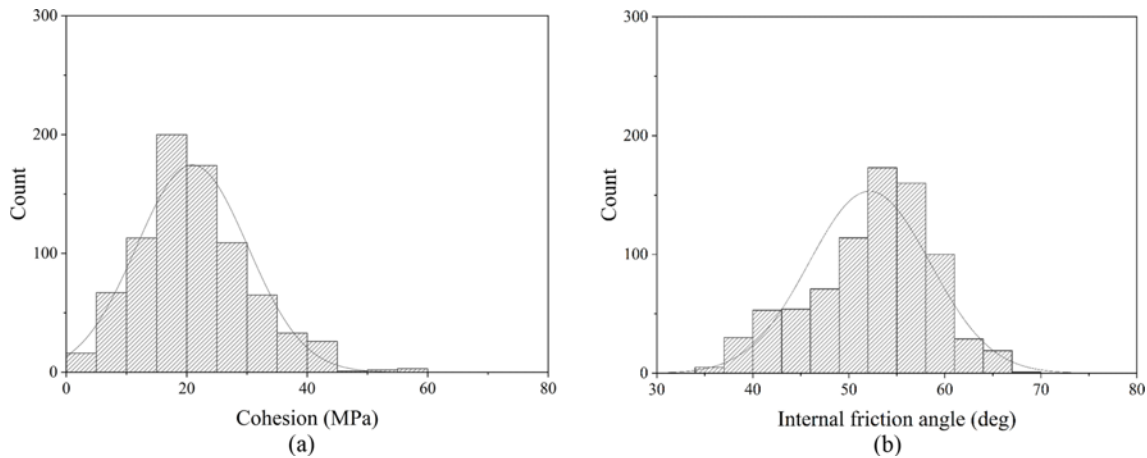


Fig. 1. Distributions of the Mohr-Coulomb Constants: (a) Cohesion, (b) Internal Friction Angle

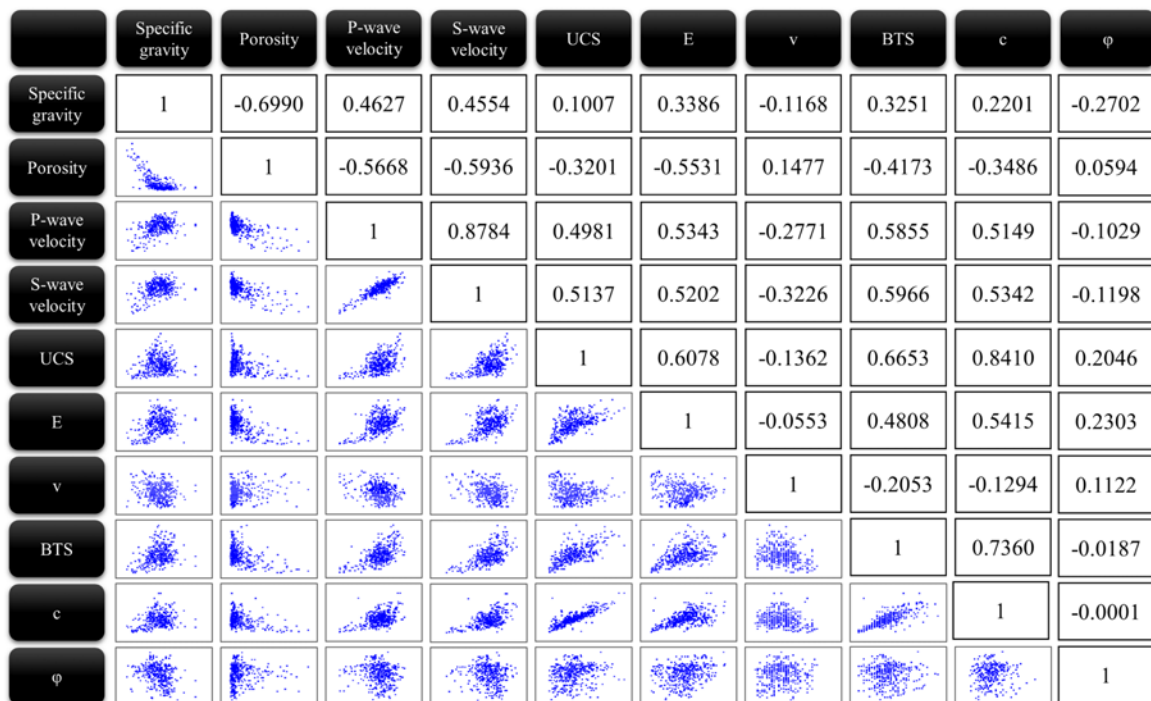


Fig. 2. Correlation Matrix between the Intact Rock Properties

results of the dependent properties.

The distributions of the Mohr-Coulomb constants, which are the main prediction targets of this study, are shown in Fig. 1. Histograms and normal distribution curves are shown, not taking rock type into consideration. Cohesion exhibited some normality, however, KS test results revealed that it could not assume a normal distribution at a significance level of 0.05 (Fig. 1(a)). The internal friction angle could not be assumed to be a normal distribution either, exhibiting a somewhat skewed tendency.

The correlation matrix is presented in Fig. 2 to investigate the correlation between the variables. The numeric value in the matrix denotes the correlation coefficient. The cohesion had the highest correlation with the uniaxial compressive strength (0.8410), followed by the Brazilian tensile strength (0.7360). The Poisson's

ratio, specific gravity, and porosity had low correlations with the cohesion, while the others exhibited similar levels. On the other hand, the internal friction angle did not have meaningful correlations. Though specific gravity exhibited the highest correlation (-0.2702), which was very weak, the others had even lower correlations.

4. Prediction Results and Discussion

4.1 XGB Model Construction and Performance Evaluation

The database used in this study consisted of eight features (independent variables) and two labels (dependent variables), and the total number of datasets was 809. Two labels, i.e., cohesion and internal friction angle, had very weak correlations with each

Table 3. Hyperparameters in the XGB Model Used in This Study

Hyperparameter	Meaning	Cohesion		Internal friction angle	
		Range	Optimal value	Range	Optimal value
N_estimator	Number of trees or basic learner	[100 – 2,000]	1,000	[100 – 2,500]	2,500
Learning_rate	Learning rate	[0.01 – 0.30]	0.01	[0.01 – 0.30]	0.01
Max_depth	Maximum depth or number of split	[3 – 10]	10	[3 – 20]	15
Subsample	Subsampling ratio for training a tree	[0.1 – 1.0]	0.1	[0.1 – 1.0]	0.5

other so that two independent XGB models were established for each label. Python code, the scikit-learn package, and the XGBoost package were used to construct the models and control the entire learning procedure.

A total of 70% of the database was randomly selected for training the model, and the remaining 30% was used as the testing set. In regression and/or classification applications using machine learning, it is crucial to set proper hyperparameter values such that the model performs well in terms of effectiveness and precision. Some important hyperparameters of the XGB model are listed in Table 3. The optimal values for each parameter were selected by a grid search within this range. A five-fold cross validation was adopted through the parameter tuning procedure.

Though other hyperparameters, such as `colsample_bytree`, and `reg_lambda`, need tuning, the number of features used in this study was not large, so that the default values for the others, which are not listed in Table 3, were assigned.

The prediction performance of the models was evaluated. The prediction results from the testing set and corresponding actual results were compared using the root mean squared error (RMSE). Meanwhile, these two results were plotted in a 1-1 graph, and the R^2 values from a linear fit line were calculated. Two evaluators, that is, RMSE and R^2 , can be expressed as Eqs. (5) and (6), respectively:

$$RMSE = \sqrt{\frac{1}{n} \sum (y - \hat{y})^2}, \quad (5)$$

$$R^2 = 1 - \frac{\sum (y - \hat{y})^2}{\sum (y - \bar{y})^2}, \quad (6)$$

where y denotes actual, measured label, \hat{y} is the predicted value, and \bar{y} is the average of y .

4.2 Prediction Result and Comparative Study

After training the XGB models through the aforementioned procedure, the prediction values were calculated using the testing set. Fig. 3 shows the comparison between the predicted and actual data with a 1-1 scale line.

The RMSE and R^2 for cohesion were calculated as 3.6807, and 0.8335, whereas those for the internal friction angle were 4.8645 and 0.4476, respectively. In the case of cohesion, the prediction performance was acceptable from an engineering perspective. However, the internal friction angle achieved less

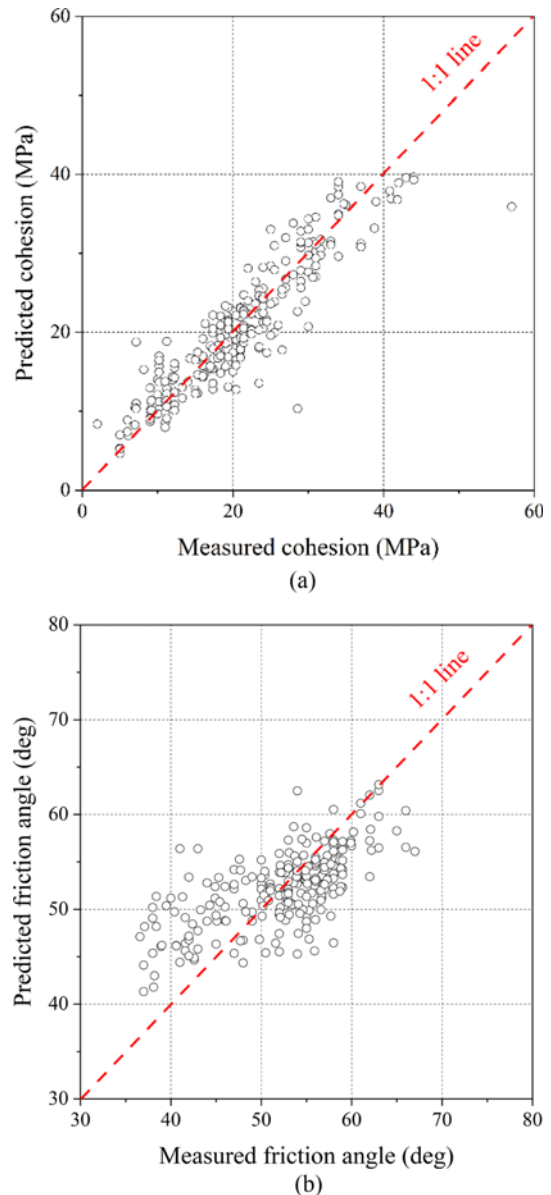


Fig. 3. Prediction Performance of the XGB Model: (a) Cohesion, (b) Internal Friction Angle

suitable results, which also could be inferred from the weak correlation between the variables shown in Fig. 2. Meanwhile, the database used in this study consisted of a wide range of experimental data, regardless of rock type and location, with the

purpose of providing broad references. Therefore, it was thought that relatively scattered result for the internal friction angle was not caused by the prediction model, but by the intrinsic variation of the input values. If the technique is applied to a database from a specific region or rock type, a better prediction would be expected.

In order to compare the performance of the XGB model, additional prediction models were established, which were conventional regression models and ANN incorporated with simulated annealing (ANN-SA). Several conventional regression models, such as single variable (SV), linear multivariable, and nonlinear multivariable models were considered, however, the prediction results did not exhibit remarkable differences, thus only SV models were tested.

As eight input variables existed, SV models were selectively investigated. Based on the correlation matrix between variables, two variables for cohesion and the internal friction angle, which had the highest correlation, were selected. In the case of cohesion, uniaxial compressive strength (0.841), and Brazilian tensile strength (0.736) were selected, and the specific gravity (-0.270), and Young's modulus (0.230) were selected for the internal friction angle. Linear, exponential, power, and logarithmic models were applied to each case, and their forms were identical for both dependent variables, as expressed in Eq. (7).

$$\begin{array}{ll} \text{Linear} & y = ax + b \\ \text{Exponential} & y = a + be^{cx} \\ \text{Power} & y = a + bx^c \\ \text{Logarithm} & y = a + b \log(x + c) \end{array} \quad (7)$$

Table 4 lists fitting constants and R^2 of each model. Note that R^2 in Table 4, which denotes conventional determination coefficient of regression model, poses a different meaning from that of Eq. (6), and missing values in Table 4 denote that the case did not converge.

In the case of cohesion, the exponential function using uniaxial compressive strength as an input variable achieved the best RMSE of 4.9882. In contrast, in the case of internal friction angle, the power function using Young's modulus had as RMSE of 6.0683. It was thought that an SV model was not applicable to

the prediction of the internal friction angle even from a practical perspective, because all the cases had too low fitness values. This trend agrees well with previous research (Karaman et al., 2015; Shen and Jimenez, 2018).

ANN-SA incorporates an SA method as a global optimization algorithm with a conventional ANN. It has been adopted in several applications, such as the prediction of principal ground motion parameters (Alavi and Gandomi, 2011), estimation of waterjet performance (Zain et al., 2011), and prediction of TBM performance (Liu et al., 2020). SA is a meta-heuristic technique suitable for global optimization (Metropolis et al., 1953). A part of the solution vector is randomly perturbed to minimize the objective function. If the perturbation makes the function better, it is accepted and even if not, it could be conditionally accepted considering a specific probability. Metropolis et al. (1953) suggested Eq. (8) as an acceptance criterion:

$$P(\Delta E) = \exp\left(-\frac{\Delta E}{k_b T}\right), \quad (8)$$

where ΔE denotes the variation of the objective function, k_b is the Boltzmann constant, T is the temperature at the calculation stage. It is known as Boltzmann probability and probabilistic hill climbing is allowed by comparing the probability and a random number within the range of [0, 1]. After training the ANN, global optimization using the SA was conducted.

The RMSE results from the XGB model, regression model with the highest performance (exponential function based on uniaxial compressive strength for cohesion, and power function based on specific gravity for internal friction angle, respectively), and ANN-SA were calculated as shown in Fig. 4, and Table 5. The RMSE values of the XGB, and ANN-SA models were average values from 10 randomly selected training and test sets, while those of the regression model were also averaged from 10 randomly selected datasets.

The XGB model exhibited the best prediction performance for cohesion and internal friction angle, followed by the ANN-SA, and regression models. Apart from the lowest average, the XGB also exhibited the lowest standard deviation from 10 repetitions, thus it was expected that the XGB could derive more

Table 4. Fitting Constants of Each Single Variable Models and Corresponding R^2 Value

Cohesion (MPa)					Internal friction angle (deg)						
		a	b	c	R^2		a	b	c	R^2	
UCS (MPa)	LI	0.124	5.188		0.707	SG (-)	LI	-17.68	99.73		0.072
	EX	-82.37	88.73	0.0012	0.708		EX	-	-	-	-
	POW	7.023	0.053	1.147	0.708		POW	58.69	-0.003	7.662	0.076
	LOG	-	-	-	-		LOG	499.8	-188.6	8.041	0.070
BTS (MPa)	LI	1.296	5.328		0.541	E (GPa)	LI	0.095	48.76		0.052
	EX	70.31	-67.97	-0.027	0.547		EX	50.05	0.274	0.047	0.073
	POW	-0.509	3.721	0.712	0.546		POW	50.65	6.5E-6	3.307	0.076
	LOG	-154.3	48.72	24.74	0.547		LOG	-	-	-	-

Note: LI, EX, POW, LOG denote linear, exponential, power, and logarithm model, respectively

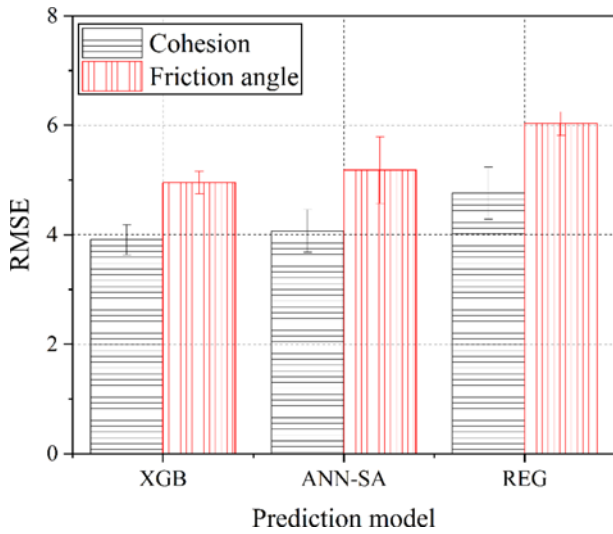


Fig. 4. RMSE Values of Each Prediction Models

Table 5. Prediction Performance of Each Models in Terms of RMSE

	Cohesion		Internal friction angle	
	Ave.	S.D.	Ave.	S.D.
XGB	3.9092	0.2756	4.9536	0.2094
ANN-SA	4.0688	0.3905	5.1806	0.6071
Regression	4.7603	0.4774	6.0307	0.2160

consistent prediction results than other models.

4.3 Sensitivity Analyses

Sensitivity analyses were performed to investigate the relative importance of eight independent variables. This importance can be inferred using several methods. For instance, the correlation coefficient in Fig. 2 also enables such an inference. Fig. 2 shows that the uniaxial compressive strength, Brazilian tensile strength, and Young’s modulus exert a strong influence on cohesion, while a remarkable effect could not be observed for the internal friction angle.

Meanwhile, algorithms based on a decision tree measure the

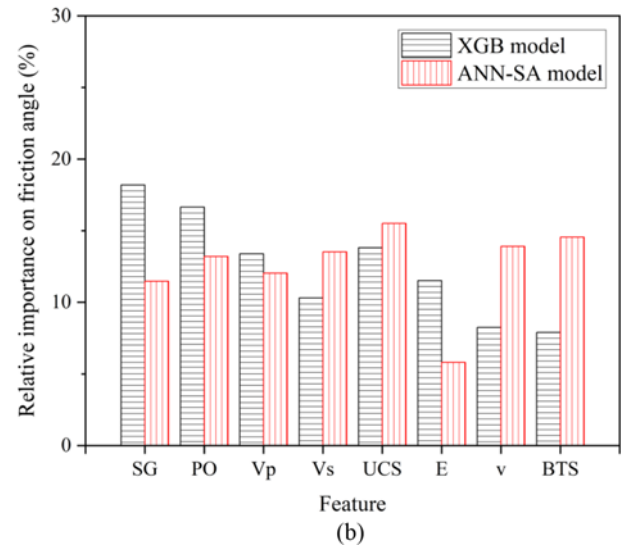
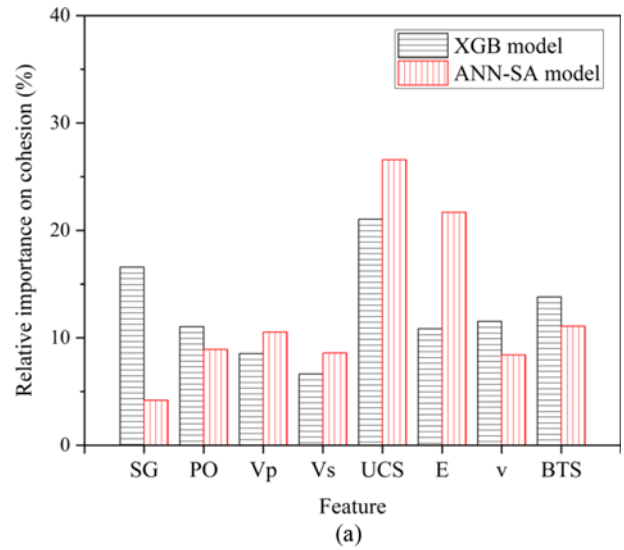


Fig. 5. Relative Importance of Each Features: (a) Cohesion, (b) Internal Friction Angle

performance or importance of individual features. Quantitative estimation, such as impurity, entropy, and information gain, is

Table 6. Sensitivity Analyses of Each Prediction Models

Feature	Cohesion				Internal friction angle			
	XGB		ANN-SA		XGB		ANN-SA	
	R.I. (%)	Rank	R.I. (%)	Rank	R.I. (%)	Rank	R.I. (%)	Rank
<i>S.G</i>	16.58	2	4.19	8	18.19	1	11.47	7
<i>PO</i>	11.04	5	8.93	5	16.64	2	13.20	5
<i>V_p</i>	8.53	7	10.53	4	13.39	4	12.04	6
<i>V_s</i>	6.63	8	8.59	6	10.30	6	13.52	4
<i>UCS</i>	21.04	1	26.59	1	13.81	3	15.51	1
<i>E</i>	10.85	6	21.68	2	11.51	5	5.80	8
<i>v</i>	11.52	4	8.41	7	8.25	7	13.91	3
<i>BTS</i>	13.80	3	11.09	3	7.90	8	14.55	2

made in each iteration, and split takes place based on the best feature, which makes the largest contribution to the tree. Therefore, the frequency or order of the split can be used as an indicator for the sensitivity analyses. The XGBoost package provides feature importance in the form of an F-score, which represents the number of splits of each feature. Similarly, the relative importance of the independent variables in the ANN can be calculated. Garson's algorithm (Garson, 1991) was adopted in this study, which calculates the contribution of each variable based on the weight matrices between input – hidden and hidden – output layers. The F-scores in the XGB model for each feature were normalized by the total score so as to compare the relative importance with the ANN-SA model. The relative importance and feature rank are shown in Fig. 5, and Table 6.

The XGB and ANN-SA models achieved relatively similar results on cohesion. The three high-rank features in the XGB model for cohesion were uniaxial compressive strength, specific gravity, and Brazilian tensile strength, while those in ANN-SA were uniaxial compressive strength, Young's modulus, and Brazilian tensile strength. The others had a similar level of importance to cohesion. On the other hand, a consistent trend could not be found in sensitivity analyses of the internal friction angle. Specific gravity, porosity, and uniaxial compressive strength were highly ranked in XGB, while uniaxial compressive strength, Brazilian tensile strength, and Poisson's ratio were highly ranked in ANN-SA, exhibiting similar levels of relative importance.

5. Conclusions

The Mohr-Coulomb failure criterion is one of the most frequently adopted models in the field of rock mechanics, and is presented by cohesion and internal friction angle. In general, these two properties are determined by triaxial compression tests, which are more time-consuming and costly than other strength tests in terms of specimens, equipment, and testing procedures. There have been numerous studies regarding the prediction of rock properties using regression models, artificial intelligence, etc. However, prediction models for Mohr-Coulomb constants are relatively fewer than those for other properties in spite of their significance. In this study, a database consisting of various rock properties collected in the southern part of the Korean Peninsula was provided, and several prediction models for the Mohr-Coulomb constants were proposed and compared.

The database was composed of 10 intact rock properties, that is, SG , PO , V_p , V_s , UCS , E , ν , BTS , c , and ϕ , and the number of data sets was 809. Before constructing the prediction models, statistical analyses were performed, such as ANOVA, to investigate its structure and characteristics.

Recently, the XGB algorithm, a kind of ensemble method, has drawn keen attention owing to its effectiveness and precision in predicting performance. Multiple basic learners in the form of a decision tree was used to construct the model and its objective function, which contains a regularization term, could derive effective and stable prediction results. Independent models for

each label were constructed and trained. Thereafter, the prediction performance was evaluated by the RMSE, and R^2 of the fitting line. The results revealed that the RMSE and R^2 for cohesion were calculated as 3.6807 and 0.8335, while those for the internal friction angle were 4.8645 and 0.4476, respectively. In the case of cohesion, the prediction performance was acceptable from an engineering perspective, while the prediction model for the internal friction angle was less suitable.

In order to compare the performance of the XGB model, a regression model with SV and ANN-SA were established. Among them, the regression model achieved the lowest performance on both dependent variables. Comparisons between XGB and ANN-SA showed that XGB model had the best performance in terms of RMSE average and standard deviation, implying that it could deduce the most precise and consistent results within the range of the database used in this study.

Sensitivity analyses were performed to investigate the relative importance of these features. XGB is capable of providing the importance in the form of an F-score, which denotes the number of splits in the tree-forming process. The best three features for cohesion were uniaxial compressive strength, specific gravity, and Brazilian tensile strength, while those for internal friction angle were specific gravity, porosity, and uniaxial compressive strength, but they did not exhibit remarkable importance. This paper aims to provide a database regarding intact rock properties as well as prediction models for Mohr-Coulomb constants so that it is expected to be utilized as a broad reference in several rock engineering applications.

Acknowledgments

This research was financially supported by the Korea Institute of Energy Technology Evaluation and Planning (KETEP) grant funded by the Korea government Ministry of Trade, Industry and Energy (No. 20211710200010C), South Korea.

ORCID

Seungbeom Choi  <http://orcid.org/0000-0002-6267-4356>
 Hoyoung Jeong  <http://orcid.org/0000-0003-4788-0212>
 Dae-Sung Cheon  <http://orcid.org/0000-0003-1643-3428>

References

- Alavi AH, Gandomi AH (2011) Prediction of principal ground-motion parameters using a hybrid method coupling artificial neural networks and simulated annealing. *Computers and Structures* 89:2176-2194, DOI: 10.1016/j.compstruc.2011.08.019
- Armaghani DJ, Amin MFM, Yagiz S, Faradonbeh RS, Abdullah RA (2016) Prediction of the uniaxial compressive strength of sandstone using various modeling techniques. *International Journal of Rock Mechanics and Mining Sciences* 85:174-186, DOI: 10.1016/j.ijrmms.2016.03.018
- Armaghani DJ, Hajihassani M, Bejarbaneh BY, Marto A, Mohamad ET (2014) Indirect measure of shale shear strength parameters by means

- of rock index tests through an optimized neural network. *Measurement* 55:487-498, DOI: [10.1016/j.measurement.2014.06.001](https://doi.org/10.1016/j.measurement.2014.06.001)
- ASTM D7012-14e1 (2014) Standard test methods for compressive strength and elastic modulus of intact rock core specimens under varying states of stress and temperature. ASTM D7012-14e1, ASTM International, West Conshohocken, PA, USA, DOI: [10.1520/D7012-14E01](https://doi.org/10.1520/D7012-14E01)
- Beiki M, Majidi A, Givshad AD (2013) Application of genetic programming to predict the uniaxial compressive strength and elastic modulus of carbonate rock. *International Journal of Rock Mechanics and Mining Sciences* 63:159-169, DOI: [10.1016/j.ijmms.2013.08.004](https://doi.org/10.1016/j.ijmms.2013.08.004)
- Ceryan N, Okkan U, Kesimal A (2013) Prediction of unconfined compressive strength of carbonate rocks using artificial neural networks. *Environmental Earth Sciences* 68:807-819, DOI: [10.1007/s12665-012-1783-z](https://doi.org/10.1007/s12665-012-1783-z)
- Cevik A, Sezer EA, Cabalar AF, Cokceoglu C (2011) Modelling of the uniaxial compressive strength of some clay-bearing rocks using neural network. *Applied Soft Computing* 11:2587-2594, DOI: [10.1016/j.asoc.2010.10.008](https://doi.org/10.1016/j.asoc.2010.10.008)
- Chang C, Zoback MD, Khaksar A (2006) Empirical relations between rock strength and physical properties in sedimentary rocks. *Journal of Petroleum Science and Engineering* 51(3-4):223-237, DOI: [10.1016/j.petrol.2006.01.003](https://doi.org/10.1016/j.petrol.2006.01.003)
- Chen T, Guestrin C (2016) Xgboost: A scalable tree boosting system. Proceedings of the 22nd ACM SIGKDD international conference on knowledge discovery and data mining, August 13-17, San Francisco, CA, USA, 785-794
- Diamantis K, Gartzos E, Migiros E (2009) Study on uniaxial compressive strength, point load index, dynamic and physical properties of serpentinites from central Greece: Test results and empirical relations. *Engineering Geology* 108(3-4):199-207, DOI: [10.1016/j.enggeo.2009.07.002](https://doi.org/10.1016/j.enggeo.2009.07.002)
- Ding Z, Nguyen H, Bui XN, Zhou J, Moayedi H (2019) Computational intelligence model for estimating intensity of blast-induced ground vibration in a mine based on imperialist competitive and extreme gradient boosting algorithms. *Natural Resources Research* 29(2):751-769, DOI: [10.1007/s11053-019-09548-8](https://doi.org/10.1007/s11053-019-09548-8)
- Friedman J, Hastie T, Tibshirani R (2000) Additive logistic regression: A statistical view of boosting (with discussion and a rejoinder by the authors). *The Annals of Statistics* 28(3): 337-407, DOI: [10.1214/aos/1016218223](https://doi.org/10.1214/aos/1016218223)
- Garson GD (1991) Interpretation neural network connection weights. *Artificial Intelligence Expert* 6(4):47-51
- Hajdarwish A, Shakoor A (2006) Predicting the shear strength parameters of mudrocks. Geology Society, London, UK
- Hoek E, Diederichs MS (2006) Empirical estimation of rock mass modulus. *International Journal of Rock Mechanics and Mining Science* 43(2):203-215, DOI: [10.1016/j.ijmms.2005.06.005](https://doi.org/10.1016/j.ijmms.2005.06.005)
- Horsrud P (2001) Estimating mechanical properties of shale from empirical correlations. *SPE Drilling and Completion* 16(2):68-73, DOI: [10.2118/56017-PA](https://doi.org/10.2118/56017-PA)
- Karaman K, Cihangir F, Ercikdi B, Kesimal A, Demirel S (2015) Utilization of the Brazilian test for estimating the uniaxial compressive strength and shear strength parameters. *Journal of the Southern African Institute of Mining and Metallurgy* 115:185-192
- Khandelwal M, Martro A, Fatemi SA, Ghoroghi M, Armaghani DJ, Singh TN, Tabrizi O (2018) Implementing an ANN model optimized by genetic algorithm for estimating cohesion of limestone samples. *Engineering with Computers* 34:307-317, DOI: [10.1007/s00366-017-0541-y](https://doi.org/10.1007/s00366-017-0541-y)
- Kılıç A, Teymen A (2008) Determination of mechanical properties of rocks using simple methods. *Bulletin of Engineering Geology and the Environment* 67(2):237-244, DOI: [10.1007/s10064-008-0128-3](https://doi.org/10.1007/s10064-008-0128-3)
- Kovari K, Tisa A, Einstein HH, Franklin JA (1983) Suggested methods for determining the strength of rock materials in triaxial compression: Revised version. *International Journal of Rock Mechanics and Mining Science* 20:283-290, DOI: [10.1016/0148-9062\(83\)90598-3](https://doi.org/10.1016/0148-9062(83)90598-3)
- Liang W, Luo S, Zhao G, Wu H (2020) Predicting hard rock pillar stability using GBDT, XGBoost, and LightGBM algorithms. *Mathematics* 8:1-17, DOI: [10.3390/math8050765](https://doi.org/10.3390/math8050765)
- Liu B, Wang R, Zhao G, Guo X, Wang Y, Li J, Wang S (2020) Prediction of rock mass parameters in the TBM tunnel based on BP neural network integrated simulated annealing algorithm. *Tunnelling and Underground Space Technology* 95:1-12, DOI: [10.1016/j.tust.2019.103103](https://doi.org/10.1016/j.tust.2019.103103)
- Metropolis N, Rosenbluth AW, Rosenbluth MN, Teller AH, Teller E (1953) Equation of state calculations by fast computing machines. *The Journal of Chemical Physics* 21(6):1087-1092, DOI: [10.1063/1.1699114](https://doi.org/10.1063/1.1699114)
- Mishra DA, Basu A (2013) Estimation of uniaxial compressive strength of rock materials by index using regression analysis and fuzzy inference system. *Engineering Geology* 160:54-68, DOI: [10.1016/j.enggeo.2013.04.004](https://doi.org/10.1016/j.enggeo.2013.04.004)
- Monjezi M, Amini-Khoshalan H, Razifard M (2012) A neuro-genetic network for predicting uniaxial compressive strength of rocks. *Geotechnical and Geological Engineering* 30:1053-1062, DOI: [10.1007/s10706-012-9510-9](https://doi.org/10.1007/s10706-012-9510-9)
- Nguyen-Sy T, Vu MN, Tran-Le AD, Tran BV, Nguyen TTN, Nguyen TT (2021) Studying petrophysical properties of micritic limestone using machine learning methods. *Journal of Applied Geophysics* 184:1-9, DOI: [10.1016/j.jappgeo.2020.104226](https://doi.org/10.1016/j.jappgeo.2020.104226)
- Nicholson GA, Bieniawski ZT (1990) A nonlinear deformation modulus based on rock mass classification. *International Journal of Mining and Geological Engineering* 8(3):181-202, DOI: [10.1007/BF01554041](https://doi.org/10.1007/BF01554041)
- Qiu Y, Zhou J, Khandelwal M, Yang H, Yang P, Li C (2021) Performance evaluation of hybrid WOA-XGBoost and BO-XGBoost models to predict blast-induced ground vibration. *Engineering with Computers*
- Shen J, Jimenez R (2018) Predicting the shear strength parameters of sandstone using genetic programming. *Bulletin of Engineering Geology and the Environment* 77:1467-1662, DOI: [10.1007/s10064-017-1023-6](https://doi.org/10.1007/s10064-017-1023-6)
- Shen J, Wan L, Zuo J (2019) Non-linear shear strength model for coal rocks. *Rock Mechanics and Rock Engineering* 52:4123-4132, DOI: [10.1007/s00603-019-01775-y](https://doi.org/10.1007/s00603-019-01775-y)
- Singh VK, Singh D, Singh TN (2001) Prediction of strength properties of some schistose rocks from petrographic properties using artificial neural networks. *International Journal of Rock Mechanics and Mining Sciences* 38:269-284, DOI: [10.1016/S1365-1609\(00\)00078-2](https://doi.org/10.1016/S1365-1609(00)00078-2)
- Sonmez H, Gokceoglu C, Nefeslioglu HA, Kayabasi A (2006) Estimation of rock modulus: For intact rocks with an artificial neural network and for rock masses with a new empirical equation. *International Journal of Rock Mechanics and Mining Science* 43(2):224-235, DOI: [10.1016/j.ijmms.2005.06.007](https://doi.org/10.1016/j.ijmms.2005.06.007)
- Torabi-Kaveh T, Naseri F, Saneie S, Sarshari B (2015) Application of artificial neural networks and multivariate statistics to predict UCS and E using physical properties of Asmari limestone. *Arabian Journal of Geosciences* 8:2889-2897, DOI: [10.1007/s12517-014-1331-0](https://doi.org/10.1007/s12517-014-1331-0)
- Yesiloglu-Gultekin N, Gokceoglu C, Sezer EA (2013) Prediction of uniaxial compressive strength of granitic rocks by various nonlinear tools and comparison of their performances. *International Journal*

- of Rock Mechanics and Mining Sciences* 62:113-122, DOI: [10.1016/j.ijrmms.2013.05.005](https://doi.org/10.1016/j.ijrmms.2013.05.005)
- Zain AM, Haron H, Sharif S (2011) Estimation of the minimum machining performance in the abrasive waterjet machining using integrated ANN-SA. *Expert Systems with Applications* 38:8316-8326, DOI: [10.1016/j.eswa.2011.01.019](https://doi.org/10.1016/j.eswa.2011.01.019)
- Zhang W, Wu C, Zhong H, Li Y, Wang L (2021) Prediction of undrained shear strength using extreme gradient boosting and random forest based on Bayesian optimization. *Geoscience Frontiers* 12:469-477, DOI: [10.1016/j.gsf.2020.03.007](https://doi.org/10.1016/j.gsf.2020.03.007)
- Zhou J, Qiu Y, Armaghani DJ, Zhang W, Li C, Zhu S, Tarinejad R (2021) Predicting TBM penetration rate in hard rock condition: A comprehensive study among six XGB-based metaheuristic technique. *Geoscience Frontiers* 12:1-13, DOI: [10.1016/j.gsf.2020.09.020](https://doi.org/10.1016/j.gsf.2020.09.020)